



# Comprehensive Processing of Basalt together with Magnetite Concentrate in Order to Obtain Ferrous Alloy and Calcium Carbide

V.M. Shevko \*, G.E. Karataeva, A.D. Badikova, M.A. Tuleev, R.A. Uteeva

M. Auezov South Kazakhstan State University, Kazakhstan

\* Corresponding author: Email address: viktor.m.shevko@mail.ru

Received 07.08.2020; accepted in revised form 02.09.2020

## Abstract

This article is devoted to basalt reprocessing together with magnetite concentrate in order to obtain ferrous alloy and calcium carbide. The studies have been based on thermodynamic simulation and electric smelting in arc furnace. The thermodynamic simulation has been performed using HSC-5.1 software based on the principle of minimum Gibbs energy. The blend was smelted in arc furnaces. On the basis of the obtained results of combined processing of basalt, it has been established that under equilibrium conditions, the increase in carbon content from 36 to 42 wt % of basalt and concentrate mixture makes it possible to increase the aluminum extraction into the alloy up to 81.4%, calcium into calcium carbide – up to 51.4%, and silicon into the alloy – up to 78.5%. Increase in the amount of lime to 32% allows to increase the content of calcium carbide to 278 dm<sup>3</sup>/kg. Electric smelting of the blend under laboratory conditions in the presence of 17-32% of lime makes it possible to extract ferrous alloy containing 69.5-72.8% of silicon, 69.1-70.2% of aluminum, and to obtain ferrous alloy containing 49-53% of  $\Sigma$ Si and Al and calcium carbide in the amount of 233-278 dm<sup>3</sup>/kg. During large-scale laboratory smelting of blend comprised of basalt (38.5%), magnetite concentrate (13.4%), lime (15.4%), and coke fines (32.7%), the ferrous alloy has been produced containing 48-53% of  $\Sigma$ Si and Al, calcium carbide in amount of 240-260 dm<sup>3</sup>/kg. Extraction of Si and Al into the alloy was 70.4 and 68.6%, respectively; Ca into carbide – 60.3%; Zn and Pb into sublimates – 99.6 and 92.8%, respectively.

**Keywords:** Basalt, Ferrous alloy, Calcium carbide, Electric smelting

## 1. Introduction

Basalt is the most common magmatic rock occupying  $\approx$ 30% of the Earth surface area [1, 2]. Basalt is generally used as construction and facing material [3, 4],

Basalt is applied for stone casting (wear-resistant and heat-resistant) and is subjected to smelting using stone casting technology at a temperature of 1,100-1,450 °C [5]. There are known methods of obtaining siminals, synthetic mineral alloys from which stone-cast products (pipes, tiles) are obtained, from basalt according to the technology of stone casting with the addition of chromite ores, titanium oxide [6].

The main direction of basalt processing is the production of basalt fiber [7, 8] (for manufacturing of heat-and sound-insulating materials) [9, 10], continuous basalt fiber (for the production of, for example, basalt fabrics, nets for roadway reinforcement, basalt pipes [11], balloons, acid-resistant fittings, etc.) [12, 13], and basalt wool [14-19].

There are studies on the use of basalt as an alternative raw material for the production of Portland-cement clinker [20, 21], and as a mineral mixture for Portland cement, which reduces CO<sub>2</sub> emissions per ton of Portland cement [22].

Basalt is also used as aggregate [23-25]. Studies are known on the use of basalt aggregates in concrete (in combination with

limestone) [26] and asphalt concrete [27] mixtures, allowing to obtain more durable characteristics of concrete structures. Studies are also known on the addition of fine-grained basalt fiber to cement concrete, allowing to improve the properties of fine-grained and high-strength concretes [28], as well as on the inclusion of basalt fibers in concrete [29, 30]

Basalt powder is also used in the production of epoxy composites additionally reinforced with basalt fiber [31] and as a replacement for cement (in the production of asphalt concrete mixture) to improve the hydration of cement and mortar properties [32]. Highly dispersed basalt powders obtained by ultrasonic dispersion are used as a basis for the manufacture of samples from ceramics [33]; the technology of production of basalt ceramics from ground basalt without a binder is also known [34], as well as the production of other products [35-39].

Table 1.

 $\Delta G^0$  of reaction (1) as a function of temperature

T, K	1,473	1,673	1,773	1,973	2,073	2,092.8	2,173
$\Delta G^0$ , kJ*	713.8	486.6	410.9	137.7	22.7	0.0	-91.7

\* $\Delta G^0$  is computed using HSC-5.1 software: (Reaction Equations option) [44]

During electric smelting of basalts, steel chips are added to the blend (the amount of the chips depends on the predicted grade of ferrous alloy and Si and Al content in it). At present, steel chips are scarce materials, their cost is 9,000-14,000 RUB/t [45]. These two factors dictate necessity of substitution of steel chips for basalt reprocessing with production of ferrous alloy and calcium carbide. Such substitution can be presented by magnetite, in particular, magnetite concentrate produced by Iron Concentrate Company from floatation tailings of copper containing rocks of

Table 2

 $\Delta G^0$  of reaction (2) as a function of temperature

T, K	1,473	1,573	1,673	1,773	1,801.6	1,873	1,973	2,073
$\Delta G^0$ , kJ*	1,121.3	778.5	437.1	96.8	0.0	-242.2	-572.9	-900.3

\* $\Delta G^0$  is computed using HSC-5.1 software: (Reaction Equations option) [44]

The article presents the experimental results of production of ferrous alloy, calcium carbide from Daubaba basalt using magnetite concentrate. The novelty of the studies is in analysis of substitution of expensive steel chips with magnetite concentrate during smelting of basalt for production of ferrous alloy and calcium carbide.

## 2. Methods

The studies were performed by thermodynamic simulation using HSC-5.1 software based on the minimum of Gibbs energy ( $\Delta G^0$ ) [44] and smelting in electric arc furnace. The first stage of thermodynamic simulation was devoted to determination of the influence of temperature and quantitative weight distribution (kg) of substances in the considered system.

An algorithm was developed to calculate the equilibrium degree of distribution of elements among substances ( $\alpha_e$ , %) [47], according to which, using data on the quantitative distribution of substances obtained using the Equilibrium Compositions software

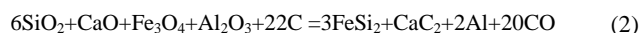
For the complex processing of basalts, the authors have created a new technology for the simultaneous production of two types of products – ferroalloy (containing aluminum and silicon) and calcium carbide – from Kazakhstan basalts, which are currently obtained by various electrothermal methods. Combining the simultaneous production of ferroalloy and calcium carbide will reduce energy consumption by reducing heat losses by the furnace unit and will increase the level of complex processing of raw materials [40-43]. The technology is based on the following reaction:



which in terms of thermodynamics is possible at  $>2,092.8\text{K}$  (Table 1).

Sayak and Shatyrol deposits at Balkhash beneficiation plant [46]. The iron content is 58-64%.

In the presence of magnetite, combined formation of iron silicide, calcium carbide, and aluminum occurs at  $>1,801.6\text{K}$  as follows (Table 2):



module of the HSC-5.1 complex, the equilibrium degree of distribution of elements ( $\alpha_e$ , %) was calculated from the ratio of the mass of the element (kg) in the product ( $G_{\text{El}(\text{pr})}$ ) to the mass of the element (kg) in the original system ( $G_{\text{El}(\text{ref})}$ ) according to the formula:

$$\alpha_e = \frac{G_{\text{El}(\text{pr})}}{G_{\text{El}(\text{ref})}} \cdot 100 \quad (3)$$

The calculation of the mass of an element (El) in the initial mixture ( $G_{\text{El}(\text{ref})}$ ) was carried out according to the formula:

$$G_{\text{El}(\text{ref})} = \frac{x_{\text{AEl}}}{M_i} \cdot G_i \quad (4)$$

where  $A_{\text{El}}$  was the atomic mass of the element in the original substance

$M_i$  was the molecular weight of the starting material

$G_i$  was the mass of the initial substance, kg

$x$  was the number of kilo-atoms of an element in the original substance

Calculation of the mass of an element (EI) in the interaction products ( $G_{EI (pr)}$ ), kg, was produced by the formula:

$$G_{EI (pr)} = (nA_{EI}) / M_{i (pr)} \cdot G_{i (pr)} \quad (5)$$

where

$A_{EI}$  was the atomic mass of the element in the product

$M_{i (pr)}$  was the molecular weight of the product substance.

$G_{i (pr)}$  was the mass of the substance in the product, kg

$n$  was the number of kilo-atoms of a substance element in the product.

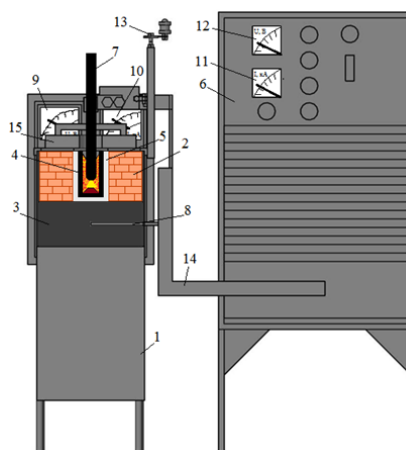
After finding  $G_{EI (pr)}$  and  $G_{EI (ref)}$ , the calculation of the equilibrium degree of distribution of the elements by substances was carried out according to the formula (3).

Upon thermodynamic simulation, the basalt/magnetite concentrate ratio in the blend was 3. Such ratio allowed to obtain ferrous alloy where  $\sum Si$  and Al was 55%. The carbon content was 100% of theoretically required for recovery of Fe, Si and Al to elemental form, and of Ca – to  $CaC_2$ .

The experimental facility for laboratory scale smelting is illustrated in Fig. 1.



I



II

Fig. 1. One-electrode laboratory electric arc furnace: 1 - furnace shell, 2 - chromomagnesite lining, 3 - carbon graphite bottom, 4 - graphite crucible, 5 - carbon graphite bed, 6 - TDZhF-1002 transformer, 7 - graphite electrode, 8 - lower current conductor, 9-12 - control ammeters and voltmeters, 13 - electrode moving mechanism, 14 - flexible portion of short circuit, 15 - furnace cover; I - general view, II - schematic view of furnace with components

The blend was smelted in one-electrode arc furnace lined with chromomagnesite bricks. Bottom electrode was made of graphite block. A graphite crucible ( $d = 6$  cm,  $h = 12$  cm) was installed on the bottom. The space between the crucible and lining was filled with graphite fines. The furnace top was closed with removable cover with holes for graphite electrode ( $d = 3$  cm) and gas discharge. Prior to smelting, the crucible was heated by arc during 20-25 min. Then the crucible was charged with the first batch of blend (200 g). It was smelted in 3-5 min, then the rest of the blend was charged (200 g) and smelted during the required time. The electric furnace was powered by a TDZhF-1002 transformer. The required power was maintained by thyristor. Current was controlled by a Tange 42L6 ammeter (class of precision: 1.5), voltage was controlled by a Chint 42L6 voltmeter (class of precision: 1.5). After smelting the furnace was cooled for 6 h. The graphite crucible was removed from the furnace and broken. Carbide and ferrous alloy were weighed and analyzed for Fe, Si, Ca, and Al. Prior to blending, ore, coke, lime, quartzite were decomposed to particle size of 0.5-1.5 cm and dried at 120°C. The electric mode of smelting is shown in Table 3.

Large-scale laboratory tests were performed at the Chair of Metallurgy, in Auezov South Kazakhstan State University. The ore was processed with production of calcium carbide, ferrous alloy, and zinc sublimates in a single-phase electric furnace

powered by a TDZhF-1002 transformer, 56 kVA (maximum current: 1,200 A, voltage: 56 V) (Fig. 2).



Fig. 2. Large-scale laboratory electrothermal assembly

The furnace was lined with chromomagnesite, with carbon graphite bottom. The furnace bath was rectangular: 0.2×0.2 m; height was 0.26 cm; capacity was 0.0104 m<sup>3</sup>. The bottom was inclined to tap opening of 8°. The lining was enclosed into steel shell with the thickness of 1.5 mm. The space between the shell and lining was filled with two asbestos sheets with the thickness of 0.8 cm (each). In the upper part of the lining, a cover was installed (chromomagnesite in metal shell). The cover height was 9 cm, opened by two rods. Electrode was in into the furnace via a hole in the cover with the diameter of 9 cm. Graphitized electrode was used. Electrode diameter was 7 cm. Electrode support and power supply were combined. Electrode with support mechanism was moved by screw. Furnace power was adjusted from 0 to 35 kVA by thyristor located in the TDZhF-1002 transformer. Power was supplied to the carbon graphite bottom from the transformer using three copper rods. Current was adjusted by a TENGGEN 42L6 GB/T7676-1998 ammeter, and voltage – by a CHNT 4226 voltmeter (China).

The temperature at the top was measured by a TPP-0679 886 thermocouple and recorded by a METAKON RS-485 instrument. The furnace bottom was cooled by a coil (10 tubes, diameter: 2 cm each). The tubes were filled with water at 20-22°C.

The furnace was preheated for 4.5-5 h by arc. The prepared blend was charged into the furnace in batches: 5 kg initially and 5 kg after smelting in batches. The furnace was preheated for 4.5-5 h by arc. The electrical smelting regime is shown in Table 3.

Table 3.

Electrical parameters of basalt electric smelting

Types of smelting	Current, A	Voltage, V
Laboratory		
Furnice firing	250-300	45-50
Furnice blend smelting	350-450	20-30
Enlarged laboratory		
Furnice firing	600-700	45-50
Furnice blend smelting	700-900	30-40

Carbide formation in the furnace was determined by melt sampling. The melt was tapped via opening with the diameter of 2.5 cm into casting mold (28×8×9 cm).

Prior to melt tapping, the opening was cleaned with breaker and processed by burning. After tapping of ferrous alloy and carbide into the mold, it was conveyed by hook to preliminary cooling (in 1-1.5 h), then the mold was finally cooled. After the cooling, the mold content was separated into alloy and calcium carbide. In order to collect samples of zinc sublimates, a special metal trap was installed before gas duct.

Analysis of raw materials and final products was performed using a JEOL JSM-6490LM scanning electron microscope (Japan), as well as by atomic adsorption method using an AAS-IN instrument (Germany) (the error of analysis for SEM was <1%, and for AAS-IN: <0.3%). In addition to SEM, the content of Si and Al in the alloy was determined by pycnometry using its density (D, g/dm<sup>3</sup>). Concentration of silicon and aluminum (C<sub>Si+Al</sub>) was determined by preliminary obtained equations [48]:

$$C_{Si+Al} = 690.679 - 545.783 \times D + 166.151 \times D^2 - 17.467 \times D^3 \quad (6)$$

(at D = 3.52-6.09 g/cm<sup>3</sup>)

$$C_{Si+Al} = 130.878 - 21.232 \times D + 0.859 \times D^2 \quad (7)$$

(at D = 6.09-7.859 g/cm<sup>3</sup>).

The error of determination of C<sub>Si+Al</sub> using this method was not higher than 2-2.5%. The content of elements in the analyzed substance was determined as arithmetic mean of three analyses.

The extraction rate of silicon and aluminum in the alloy was determined by the ration of metal weight in the alloy to the metal weight in the blend. The extraction rate of calcium into process calcium carbide (α<sub>Ca</sub>, %) was determined as follows:

$$\alpha_{Ca} = \frac{G_{cc} \cdot C_{CaC_2} \cdot 0.625}{G_{bas} \cdot C_{Ca(bas)} + G_{lime} \cdot C_{Ca(lime)}} \cdot 100 \quad (8)$$

where G<sub>bas</sub>, G<sub>lime</sub>, and G<sub>cc</sub> were the weights of basalt, lime, and calcium carbide, respectively, g; C<sub>Ca(bas)</sub>, C<sub>Ca(lime)</sub> were the contents of calcium, lime in basalt, respectively, l fraction; 0.625 was the ratio of atomic weight of calcium to the atomic weight of calcium carbide; C<sub>CaC<sub>2</sub></sub> was the concentration of CaC<sub>2</sub> in process calcium carbide, l fraction, determined as follows [49]:

$$C_{CaC_2} = L / 372 \quad (9)$$

where L was the content of calcium carbide (dm<sup>3</sup>/kg), 372 was the volume of acetylene extracted upon decomposition of calcium carbide by water according to the reaction: CaC<sub>2</sub>+H<sub>2</sub>O=C<sub>2</sub>H<sub>2</sub>+Ca(OH)<sub>2</sub>.

Content of calcium carbide was experimentally determined upon decomposition of calcium carbide by water according to the formula:

$$L = \frac{(p - p_1) \times 273 \times V}{(273 + t) \times 760 \times G} \quad (10)$$

where p and p<sub>1</sub> were the ambient pressure and elasticity of water vapors during testing, mm Hg; V was the volume of extracted acetylene, ml; G was the calcium carbide sample, g; t was the temperature, °C; L was the content of calcium carbide, dm<sup>3</sup>/kg.

Measurement error did not exceed 1-1.5%.

Figure 3 and Table 4 show elemental composition of Daubaba basalt determined by scanning electron microscopy, and Fig. 4 illustrates thermograms of Daubaba basalt. It follows from Fig. 4 that upon uniform heating of Daubaba basalt to 1,000°C, the weight loss is 10.9%. The weight loss is related with thermal destruction of mineral rocks with extraction of H<sub>2</sub>O (5%), CO<sub>2</sub> (3.65%), and OH (2.25%). Basalt is comprised of the minerals: nontronite (50%), quartz (≈10%), calcite (8.3%), thermally inertial substances (Fe<sub>2</sub>O<sub>3</sub>, MgO, CaO, FS (feldspar, albite), PFS (potassium feldspar) and others) (≈30%).

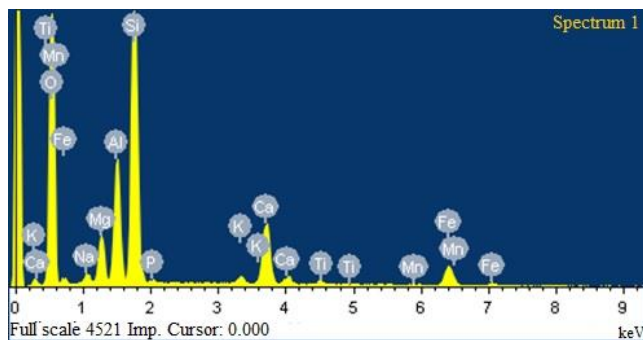


Fig. 3. Energy dispersion spectra of Daubaba basalt

Table 4.

Elemental composition of Daubaba basalt determined by SEM

Element	Si	Ca	Fe	Mg	Al	Mn	O	Na	P	K	Ti
wt %	19.62	6.68	5.57	3.63	8.61	0.24	53.03	1.14	0.28	0.74	0.46

Figure 5 illustrates X-ray phase analysis of Daubaba basalt, it follows that basalt is comprised of 51.8% nontronite ((Fe,Al)Si<sub>2</sub>O<sub>5</sub>(OH)·H<sub>2</sub>O), 16.6% calcite (Ca(CO<sub>3</sub>)), 13.1%

magnioferrite (MgFe<sub>2</sub>O<sub>4</sub>), 6.9% quartz (SiO<sub>2</sub>), 6.5% albite (FS) (Na(AlSi<sub>3</sub>O<sub>8</sub>)), 5.1% PFS (KAlSi<sub>3</sub>O<sub>8</sub>).

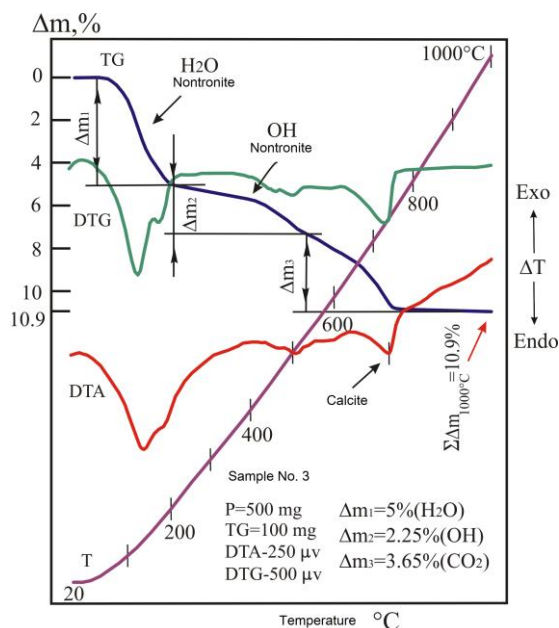


Fig. 4. Thermogram of Daubaba basalt

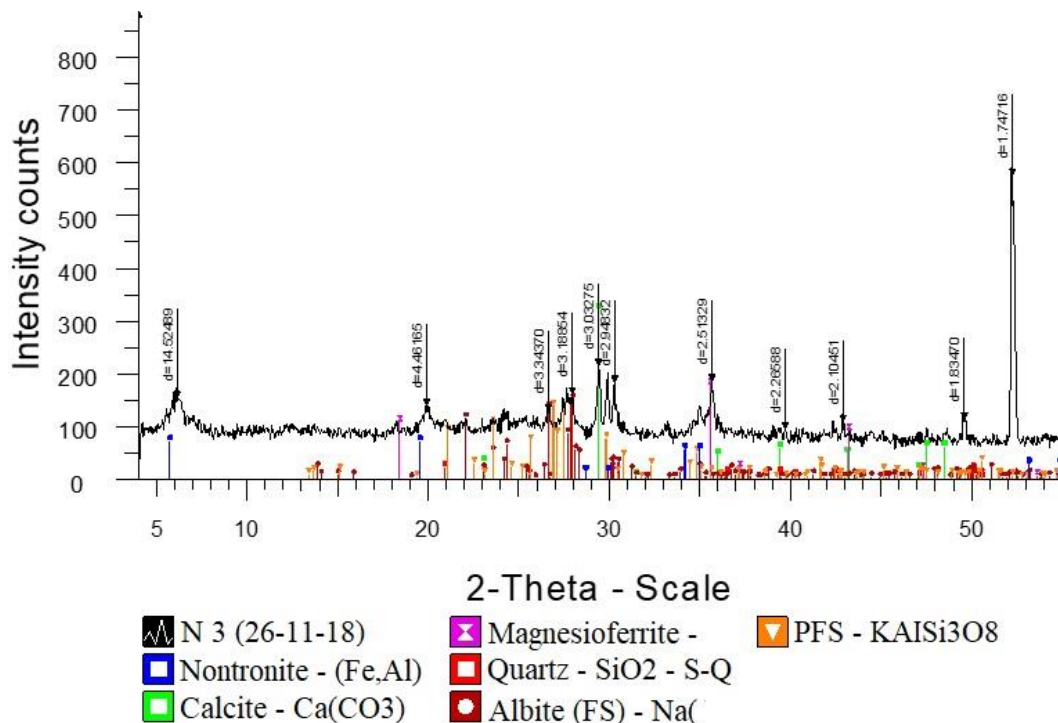


Fig. 5. X-ray phase analysis of Daubaba basalt

The following raw materials were used in the work:

- Daubaba basalt (50.2% SiO<sub>2</sub>, 18.6% Al<sub>2</sub>O<sub>3</sub>, 9.7% Fe<sub>2</sub>O<sub>3</sub>, 9.3% CaO, 6.8% MgO, 3.5% ΣK<sub>2</sub>O and Na<sub>2</sub>O, 1.5% rest);
- magnetite concentrate (85.9% Fe<sub>3</sub>O<sub>4</sub>, 9.4% SiO<sub>2</sub>, 1.2% Al<sub>2</sub>O<sub>3</sub>, 1.8% CaO, 0.2% ZnO, 0.1% PbO, 1.1% rest (MgO, Na<sub>2</sub>O, K<sub>2</sub>O, SO<sub>3</sub>, MnO);
- -coke fines (85.6% C, 4.8% SiO<sub>2</sub>, 1.6% CaO, 0.5% MgO, 1.9% Al<sub>2</sub>O<sub>3</sub>, 2.4% Fe<sub>2</sub>O<sub>3</sub>, 0.7% S, 1.2% H<sub>2</sub>O, 1.7% rest);
- lime (CaO+MgO >90%, CO<sub>2</sub> <7%).

### 3. Results and Discussion

Figure 6 illustrates quantitative distribution of substances containing silicon, aluminum, iron, and calcium. It can be seen that silicon is distributed among FeSi, FeSi<sub>2</sub>, SiO<sub>g</sub>, Fe<sub>3</sub>Si, SiC, K<sub>2</sub>SiO<sub>3</sub>, Na<sub>2</sub>SiO<sub>3</sub>, MgSiO<sub>3</sub>, SiO<sub>2</sub>; aluminum – among Al<sub>2</sub>O<sub>3</sub>, Al, and Al<sub>g</sub>; calcium – among CaSiO<sub>3</sub>, CaC<sub>2</sub>, Ca<sub>g</sub>, CaO; iron – among

Fe, Fe<sub>2</sub>O<sub>3</sub>, Fe<sub>3</sub>O<sub>4</sub>, FeSi, FeSi<sub>2</sub>, Fe<sub>3</sub>Si, 2FeO\*SiO<sub>2</sub>. It follows from Fig. 6 that formation of the targeted products (silicides of Fe, Al, CaC<sub>2</sub>) starts at 1,300°C, 1,600°C, 1,700°C, respectively. Unwanted formation of SiO<sub>g</sub> starts at 1,600°C. Figure 7 illustrates quantitative distribution of Zn and Pb as a function of temperature, it can be seen that Zn and Pb transit into gas completely at 800 and 1,300°C, respectively.

Figure 8 illustrates equilibrium distribution of Si, Fe, Al in basalt-magnetite concentrate-carbon system as a function of temperature (100% of theoretically required). It can be seen in Fig. 8(I) that with the increase in the temperature from 1,300 to 1,700°C, the rate of transition of Si into FeSi sharply increases (from 0.16 to 45.6%). Then (up to 2,100°C) the increase is less significant. Noticeable unwanted formation of SiO<sub>g</sub> takes place at T ≥ 1,900°C. Iron in the system is in elemental state (by 99.48-100%) in the range of 900-1,300°C. Then it transits into Fe<sub>3</sub>Si and, mainly, into FeSi (Fig. 8(II)).

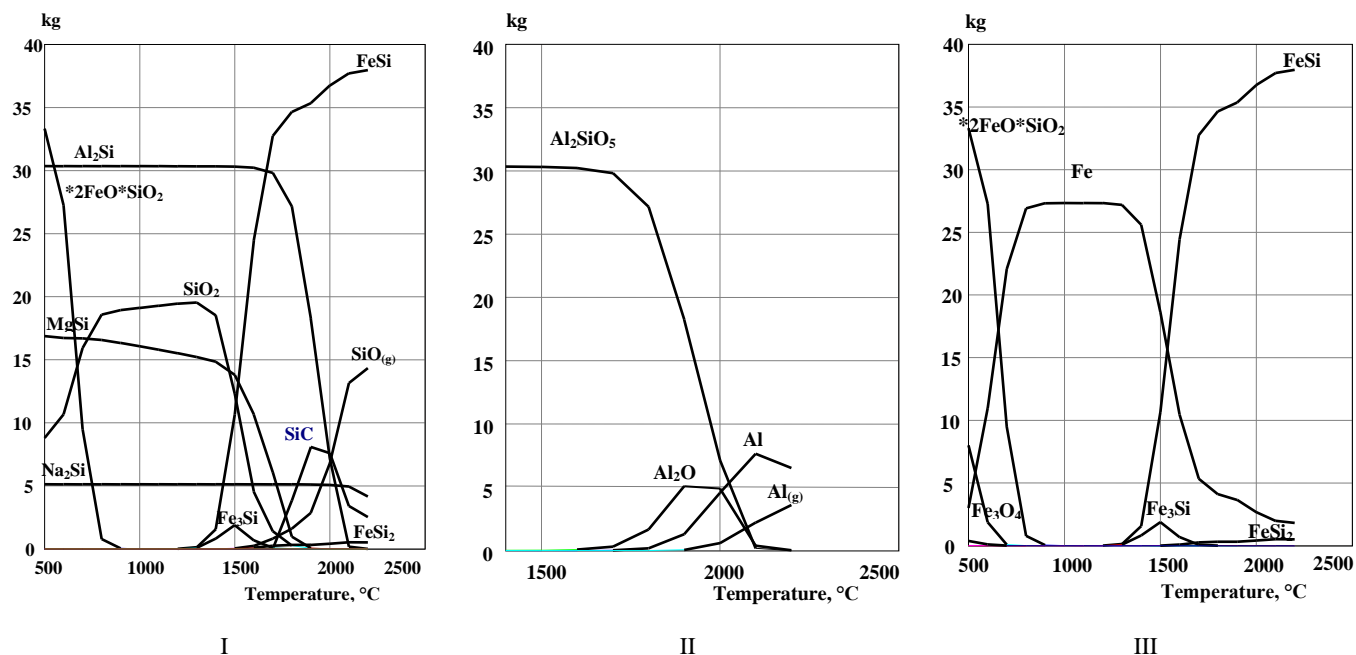


Fig. 6. Quantitative equilibrium distribution of substances containing silicon (I), aluminum (II), and iron (III) in basalt–magnetite concentrate–carbon system as a function of temperature

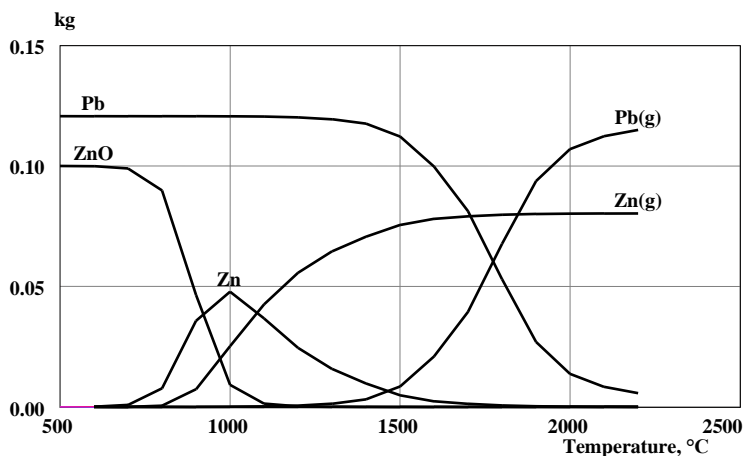


Fig. 7. Quantitative equilibrium distribution of substances containing zinc and lead) in basalt–magnetite concentrate–carbon system as a function of temperature

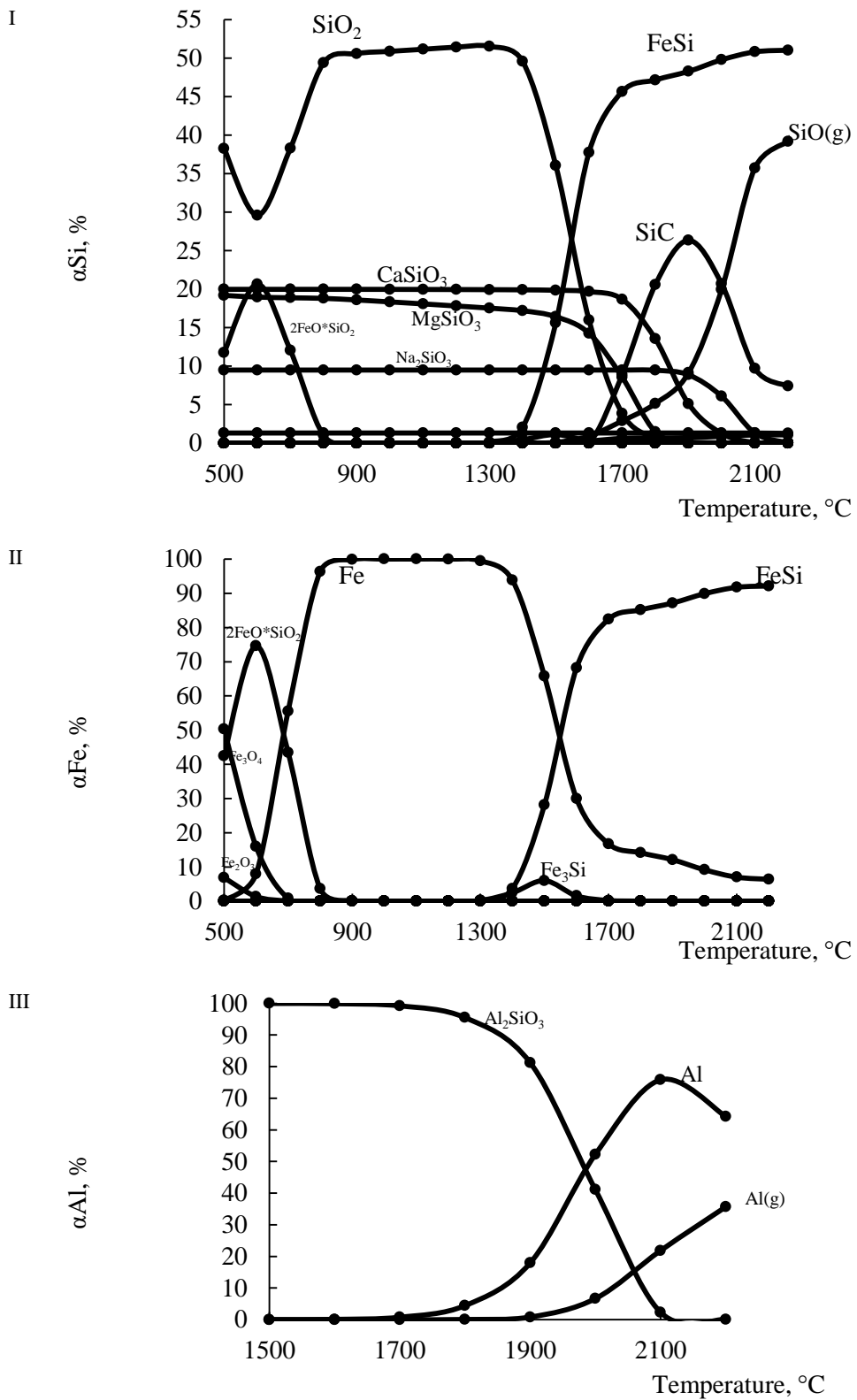


Fig. 8. Equilibrium distribution of silicon (I), iron (II), and aluminum (III) in basalt–magnetite concentrate–carbon system as a function of temperature

Aluminum is recovered from  $\text{Al}_2\text{SiO}_5$  and from  $\text{Al}_2\text{O}$  in the range of 1,800-2,200°C (Fig. 8(III)). Maximum of this process is observed at 2,100°C (75.6%). Noticeable formation of unwanted gaseous aluminum is observed at  $T \geq 1,900^\circ\text{C}$ . It should be mentioned that in the considered system, the rate of Ca transition from the blend to  $\text{CaC}_2$  does not exceed 30% (28.9 at 2,000°C),

which is attributed to its significant transition into gaseous calcium. The influence of temperature on equilibrium transition of nonferrous metals into targeted gaseous phase is summarized in Table 5. It can be seen that zinc is sublimated better than lead. In the range of 1,800-2,000°C, zinc transits into gas by 99.3-99.8%, and lead – by 60.1-88.7%.

Table 5.

Equilibrium transition of nonferrous metals into gaseous state as a function of temperature (%)

Metal	Temperature, °C											
	900	1,000	1,100	1,200	1,300	1,400	1,500	1,600	1,700	1,800	1,900	2,000
Zn	7.1	27.9	49.5	66.4	78.3	86.6	93.6	97.1	98.6	99.3	99.6	99.8
Pb	<0.01	<0.1	0.1	0.4	0.9	2.3	6.6	17.8	36.4	60.1	79.0	88.7

In order to present the influence of carbon on the considered processes, the studies were performed with 36 and 52 wt % carbon of basalt and magnetite concentrate mixture. The obtained results are illustrated in in Fig. 9. It can be seen that increase in carbon content from 36 to 52 wt % of basalt and magnetite concentrate makes it possible to increase the formation degree of

elemental aluminum from 56% to 81.4% at 2,100°C, silicon - from 62.3 to 78.5%, and transition of calcium into  $\text{CaC}_2$  - from 20.3 to 51.4%. Reduced extraction of aluminum and calcium can be attributed to evaporation of aluminum and decomposition of  $\text{CaC}_2$ :  $\text{CaC}_2 = \text{Ca}_g + 2\text{C}$  with formation of gaseous calcium.

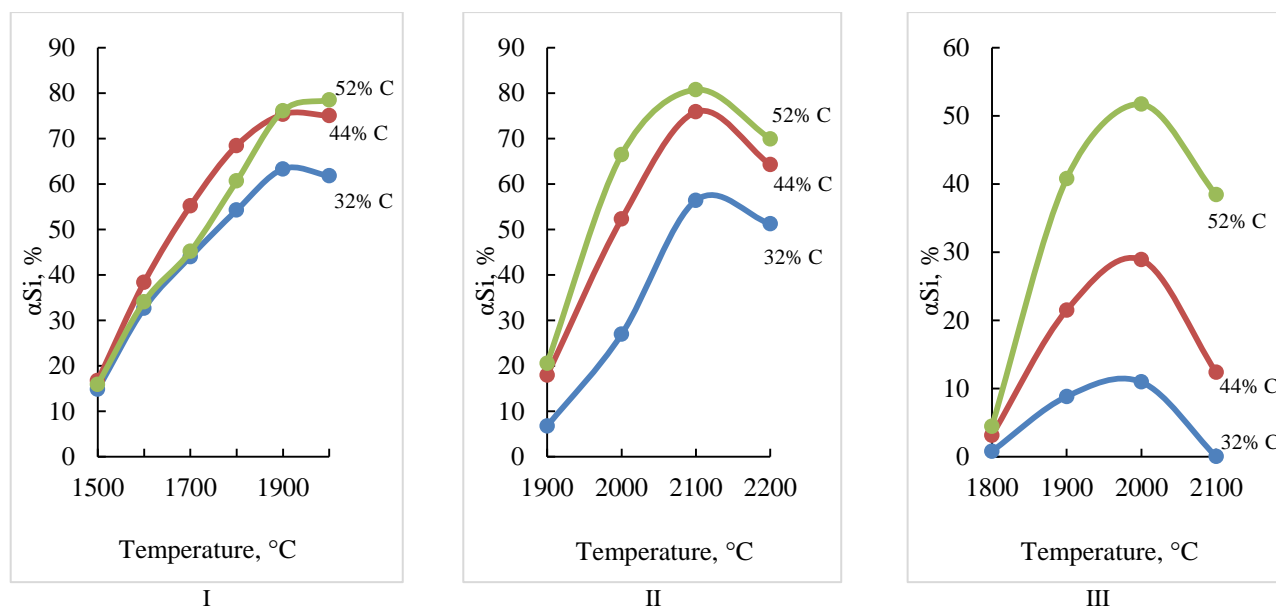


Fig. 9. Equilibrium distribution of Si (I), Al (II) in ferrous alloy, Ca in calcium carbide (III) as a function of temperature and carbon content

It follows from Fig. 9 that upon combined recovery of silicon, aluminum, and calcium, the restricting factor is transition of calcium into  $\text{CaC}_2$ , its maximum generation requires for 2,000°C and 52 wt % of C of basalt and concentrate mixture. Herewith, transition of 78.5% of Si and 66.4% of Al into the alloy should be expected.

Table 6 summarizes the influence of temperature and carbon content on concentration of Si, Al, and  $\Sigma\text{Si}$  and Al in the ferrous alloy.

As can be seen in Table 6 at 1,900-2,000°C, the cumulative concentration of Si and Al in the alloy is 39.42-45.16%. It should be mentioned that the content of  $\text{CaC}_2$  in process calcium carbide at 2,000°C and 52% of C was 40.04%, its content was 148.8  $\text{dm}^3/\text{kg}$ .

Table 6.  
 Concentration of metals in ferrous alloy as a function of temperature and carbon

Carbon content, %	Metal	Temperature, °C					
		1,500	1,600	1,700	1,800	1,900	2,000
44	Si	12.96	25.38	31.89	35.20	35.94	32.87
	Al	-	0.03	0.18	0.93	3.48	9.80
	Si+Al	12.96	25.41	32.07	36.13	39.42	42.67
52	Si	12.38	23.20	28.28	33.04	35.87	33.58
	Al	-	-	0.04	0.61	3.94	11.58
	Si+Al	12.38	23.30	28.32	33.65	39.81	45.16

As a consequence of electric smelting of basalt and magnetite concentrate mixture together with 50% coke, the ferrous alloy was obtained with the content of  $\Sigma$ Si and  $\alpha$ Al of 38-42%, as well as calcium carbide in the amount of 183-192  $\text{dm}^3/\text{kg}$ . According to [50], the produced calcium carbide was not marketable. Hence, it could attract limited interest for production of acetylene. Such carbide can be used in vegetable production [51, 52]. Upon addition of 60-120 kg of calcium carbide per 1 ha of podzol soil (soil of coniferous and mixed forests, formed in conditions of excessive moisture [53]), the cucumber yield increases by 30-50% (sometimes even up to 94%) [54].

In order to increase the content of calcium carbide during smelting of basalt and magnetite concentrate, the authors analyzed the influence of lime on the process specifications. The obtained results are illustrated in Fig. 10.

It can be seen in Fig. 10 that increase in the lime content from 0 to 32wt % of basalt and magnetite concentrate mixture leads to increase in the content of process calcium carbide from 190 to 278  $\text{dm}^3/\text{kg}$  and from 70.2 to 69.1%. In order to produce marketable calcium carbide with the content of  $\geq 233 \text{ dm}^3/\text{kg}$ , the lime content should be from 17 to 32 wt % of basalt and magnetite concentrate mixture. The boundary values of  $\alpha$ Si, L, and  $\alpha$ Al are determined by the *abcdef* plane.

Table 7 summarizes process specifications in boundary points of the *abcdef* plane in Fig. 10.

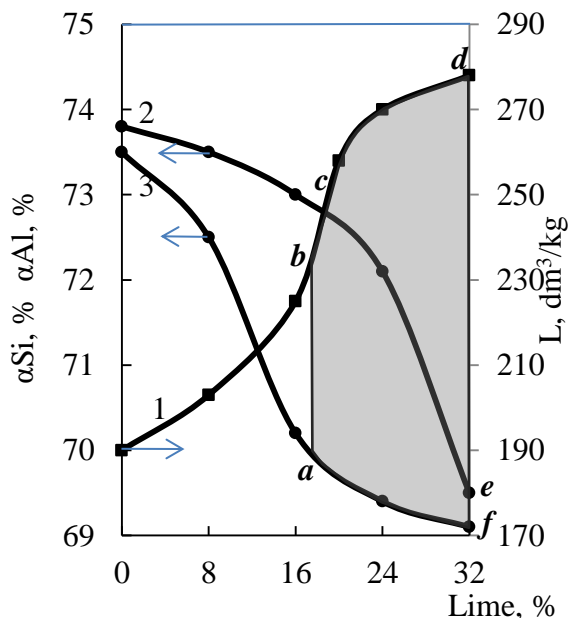


Fig. 10. Smelting specifications of basalt and magnetite concentrate mixture as a function of lime content. 1- L,  $\text{dm}^3/\text{kg}$ , 2-  $\alpha$ Si, %, 3-  $\alpha$ Al, %, abc- points on the line with 17% of lime, def- points on the line with 32% of lime

Table 7.  
 Boundary specifications of *abcdef* plane

Line in Fig. 10	Specifications			
	Lime, %	$\alpha$ Si, %	$\alpha$ Al, %	L, $\text{dm}^3/\text{kg}$
<i>abc</i>	17.0	72.8	70.2	233
<i>def</i>	32.0	69.5	69.1	278

The concentration of  $\Sigma$ Si and Al in ferrous alloy during electric smelting with 17% of lime was 52-53%, and with 32% of lime – 49-51%.

Large-scale laboratory electric smelting was performed with 52 kg of blend comprised of 38.5% of basalt, 13.4% of magnetite concentrate, 15.4% of lime, and 32.7% of coke fines. The

smelting was performed at 20-40 V and 600-800 A. The produced ferrous alloy and calcium carbide are illustrated in Fig. 11. By means of pycnometry, it was revealed that the ferrous alloy contained 48-53% of  $\Sigma$ Si and Al. Using SEM, it was determined that it contained 33.37% of Si and 12.3% of Al (Fig. 12).



I



II

Fig. 11. Products of electric smelting: I - ferrous alloy, II - calcium carbide (fragment)

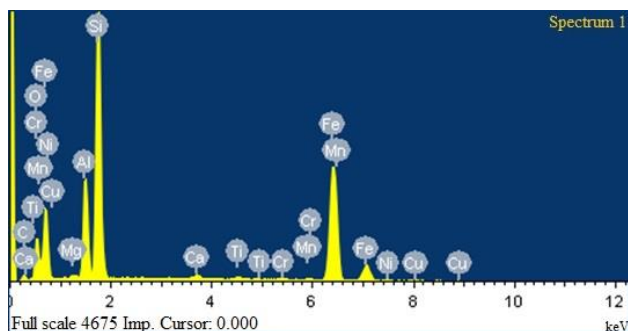


Fig. 12. SEM microscopy of ferrous alloy

Element	%	Element	%
Mg	0.36	Cr	0.17
Al	12.30	Mn	0.44
Si	33.37	Fe	51.97
Ca	0.65	Ni	0.00
Ti	0.50	Cu	0.23

The main specifications of electric smelting of basalt and magnetite concentrate mixture during large-scale laboratory tests are shown in Table 8.

Table 8.

Main technological indicators of electric smelting

Indicator	Indicator value
<i>Degree of extraction</i>	
silicon into ferrous alloy	70.4%
aluminum into ferrous alloy	68.5%
calcium into carbide	60.3%
zinc into sublimates	99.6%
lead into sublimates	92.8%
<i>Content</i>	
silicon in ferrous alloy	39-42%
aluminum in ferrous alloy	9-12%
calcium in calcium carbide	66-69%
<b>Calcium carbide content</b>	240-260 dm <sup>3</sup> /kg
<i>Product content per 1 t of basalt</i>	
ferrous alloy	0.623 t
calcium carbide	0.51 t
<i>Electric power consumption</i>	
as per 1 t of ferrous alloy	4,900-5,100 kWh
as per 1 t of calcium carbide	3,500-3,600 kWh

The obtained ferrous alloy can be classified as complex ferrous alloy: aluminum ferrosilicon [55], and the calcium carbide – as a product of the first and the second grade [50].

## 4. Conclusion

On the basis of combined reprocessing of basalt in the presence of magnetite concentrate, it is possible to conclude as follows:

- under equilibrium conditions, the increase in carbon content from 36 to 42 wt % of basalt and concentrate makes it possible to increase the extraction rate of aluminum into the alloy up to 81.4%, calcium into calcium carbide – up to 51.4%; and silicon into the alloy – up to 78.5%; lime in the blend (from 0 to 32%) makes it possible to increase the content of calcium carbide from 190 to 278 dm<sup>3</sup>/kg.
- electric smelting of the blend under laboratory conditions in the presence of 17-32% of lime makes it possible to extract into the ferrous alloy 69.5-72.8% of silicon, 69.1-70.2% of aluminum; to produce ferrous alloy containing 49-53% of  $\Sigma$ Si and Al and calcium carbide in the amount of 233-278 dm<sup>3</sup>/kg;
- during large-scale laboratory smelting of blend comprised of basalt (38.5%), magnetite concentrate (13.4%), lime (15.4%), and coke fines (32.7%), the ferrous alloy has been produced containing 48-53% of  $\Sigma$ Si and Al, calcium carbide in the amount of 240-260 dm<sup>3</sup>/kg. Extraction of Si and Al into the alloy was 70.4 and 68.6%, respectively; calcium into carbide – 60.3%; Zn and Pb into sublimates – 99.6 and 92.8%, respectively.

## Acknowledgments

This work was supported by the Ministry of Education and Science of the Republic of Kazakhstan, agreement #164-15 of March 15, 2018: Combined production of ferrous alloys and calcium carbide from nonconventional raw stuff and technogenic substances containing abundant elements.

## References

- [1] Baibatsha, A.B. (2008). *Geologiya mestorozhdenii poleznykh iskopaemykh [Geology of mineral deposits]*. Almaty: KazNTU.
- [2] Godfrey Fitton, J. (2020). Basalt and Related Rocks. *Reference Module in Earth Systems and Environmental Sciences*. DOI: 10.1016/B978-0-12-409548-9.12410-8.
- [3] Ponomarev, V.B. & Rapoport, A.T. (2012). Bazal'tovye i bazal'toplastikovy materialy dlya stroitel'stva [Basalt and basal plastic materials for construction]. *Bazal'tovye tekhnologii [Basalt technologies]*. 1, 29-35.
- [4] Sivanandhini, K., Subasree, S., Preethika, R. & Meenakshi, M. (2019). Experimental Study on using Basalt as a Construction Material. *SSRG International Journal of Civil Engineering*. 6(4), 11-12.
- [5] Pisarenko, M.V. & Patrakov, Yu. F. (2017). Integrated development of deposits in the Barzas geological and economic region. *Mining Industry*. 2(132), 31-35.
- [6] Ignatova, A.M. (2012). Sinteticheskie mineral'nye splavy, poluchennye kamennym lit'em, – material nastoyashchego i budushchego [Synthetic mineral alloys produced by stone casting]. *Bazal'tovye tekhnologii [Basalt technologies]*. 1, 46-49.
- [7] Fomichev, S.V. Babievskaya, I.Z., Dergacheva, N.P., Noskova, O.A. & Krenev, V.A. (2010). Evaluation and modification of the initial composition of gabbro - basalt rocks for mineral - fiber fabrication and stone casting. *Inorganic Materials*. 46(10), 1121-1125.
- [8] Gutnikov, S.I. & Lazoryak, B.I. (2019). Effect of Nozzle Diameter on Basalt Continuous Fiber Properties. *Fibers*. 7(7), 65. DOI: 10.3390/FIB7070065.
- [9] Dahl, T., Clausen, A. & Hansen, P. (2011). The human impact on natural rock reserves using basalt, anorthosite, and carbonates as raw materials in insulation products. *International Geology Review*. 53, 894-904.
- [10] Gurev, V.V. & Svetlyakov, M.V. (2011). Teplovukoizolyatsionnye materialy iz bazal'tovykh volokon, ikh osobennosti i fizikomekhanicheskie svoistva [Heat and sound insulating materials from basalt fibers, their peculiarities and physicochemical properties]. *Vestnik MGSU*. 3-2, 128-133.
- [11] Ponomarev, V.B. & Rapoport, A.T. (2013). Effektivnost' primeneniya bazal'tovogo nepreryvnogo volokna dlya proizvodstva trub iz polimernykh kompozitov [Efficiency of basalt continuous fibers for fabrication of polymer composite pipes]. *Bazal'tovye tekhnologii [Basalt technologies]*. 2, 38-42.
- [12] Vasileva, A.A. & Pavlova, M.S. (2019). Poluchenie bazal'tovogo nepreryvnogo volokna na osnove bazal'ta Vasil'evskogo mestorozhdeniya [Fabrication of basalt continuous fibers based on basalt of Vaslievskoe deposit]. *Tekhnika i tekhnologiya silikatov [Technique and technology of silicates]*. 26(4), 111-114.
- [13] Demeshkin, A.G. & Shvab, A.A. (2011). Eksperimental'noe issledovanie mekhanicheskikh svoistv nepreryvnogo bazal'tovogo volokna primenitel'no k proizvodstvu kompozitnykh materialov [Experimental studies of mechanical properties of continuous basalt fibers regarding fabrication of composite materials]. *Vestnik Samarskogo gosudarstvennogo tekhnicheskogo universiteta. Series: Physical and mathematical sciences*. 3(24), 185-188.
- [14] Korobkin, V.V., Samatov, I.B., Slyusarev, A.P., Tulemisova, Zh.S. (2017). Mineral raw materials of Kazakhstan as a basis for establishment of production mineral basalt wool and fibers. *Vestnik KRSU*. 17(1), 127-131.
- [15] Dalinkevich, A.A., Gumargalieva, K.Z., Marakhovskiy, S.S. & Soukhanov, A.V. (2009). Modern Basalt Fibrous Materials and Basalt Fiber – Based Polymeric Composites. *Journal of Natural Fibers*. 6(3), 248-271.
- [16] Gulamova, D.D., Shevchenko, V.P., Tokunov, S.G. & Kim, R.B. (2012). Use of solar power for the production of basalt - based mineral fibers. *Applied Solar Energy*. 48(1), 58-59.
- [17] Ivanitskii, S.G. & Gorbachev, G.F. Continuous basalt fibers: production aspects and simulation of forming processes. I. State of the art in continuous basalt fiber technologies. *Powder Metallurgy and Metal Ceramics*. 50, 125-129.
- [18] Pisciotta, A., Perevozchikov, B.V., Osovetsky, B.M., Menshikova, E.A. & Kazymov, K.P. (2015). Quality Assessment of Melanocratic Basalt for Mineral Fiber

- Product, Southern Urals, Russia. *Natural Resources Research*. 24(3), 329-337.
- [19] Novitskii, A. & Efremov, M. (2013). Technological aspects of the suitability of rocks from different deposits for the production of continuous basalt fiber. *Glass and Ceramics*. 69.
- [20] Sanjaasuren, R., Erdenebat, Ts., Rummyantsev, P.F. (2007). Theoretical evaluation of possibility on use basalts as aluminosilicate component in raw mix for synthesis of Portland cement clinker. Conference: The 12 th International Congress on the Chemistry of Cement, At Montreal, Canada, July.
- [21] Abd El-Hafiz, N.A., Abd El-Moghny, M.W., El-Desoky, H. M. & Afifi, A.A. (2015). Characterization and technological behavior of basalt raw materials for Portland cement clinker production. *IJISET - International Journal of Innovative Science, Engineering & Technology*. 2(7).
- [22] Mendes, T.M., Guerra, L. & Morales, G. (2016). Basalt waste added to Portland cement. *Acta Scientiarum. Technology*. 38(4), 431-436. DOI: 10.4025/actascitechnol.v38i4.27290.
- [23] Nguen, V.K. & Chumakov, L.D. (2009). Kompleksnoe ispol'zovanie bazal'tovykh zapolnitelei v betone [Integrated use of basalt fillers in concrete]. *Vestnik MGSU*. 1, 164-167.
- [24] Miichenko, I.P. (2010). *Napolniteli dlya polimernykh materialov [Fillers for polymer materials]*. Moscow: RGTU im. K.E.Tsiolkovskogo.
- [25] Sharifullin, F.S. (2015). Primenenie bazal'ta v kachestve napolnitelya dlya lakokrasochnogo materiala [Basalt as a filler for coating materials]. *Vestnik Kazanskogo tekhnologicheskogo universiteta*. 18(15), 95-97.
- [26] Ikkurthi, S., Mounika, L., Prasad, C. & Krishna, B. (2015). Experimental study on the use of basalt aggregate in concrete mixes. *International Journal of Civil Engineering*. 2(4), 37-40.
- [27] Engidasew, T.A. & Barbieri, G. (2014). Geo-engineering evaluation of Termaber basalt rock mass for crushed stone aggregate and building stone from Central Ethiopia. *Journal of African Earth Sciences*. 99(2), 581-594. DOI: 10.1016/j.jafrearsci.2013.11.020.
- [28] Chaohe, Ch., Guangfan, L., Qizhong, Sh. & Bifeng, J. (2014). Retain of fine dispersed basalt fiber reinforcement in cement matrix. *Applied Mechanics and Materials*. 584-586, 1691-1694. DOI: 10.4028/www.scientific.net/AMM.584-586.1691.
- [29] Vinotha, J. & Brindha, D. (2020). Influence of basalt fibers in the mechanical behavior of concrete—A review. *Structural Concrete*. DOI: 10.1002/suco.201900086.
- [30] Pirmohammad, S., Amani, B. & Majd Shokorlou, Y. (2020). The effect of basalt fibres on fracture toughness of asphalt mixture. *Fatigue & Fracture of Engineering Materials & Structures*. 43(7), 1446-1460. DOI: 10.1111/ffe.13207.
- [31] Matykiewicz, D., Barczewska, M., Knapska, K. & Skórczewskab, D. (2017). Hybrid effects of basalt fibers and basalt powder on thermomechanical properties of epoxy composites. *Composites Part B: Engineering*. 125, 157-164. DOI: 10.1016/J.COMPOSITESB.2017.05.060.
- [32] Dobiszewska, M., Pichor, W. & Szoldra, P. (2019). Effect of basalt powder addition on properties of mortar. *MATEC Web of Conferences*. Krynica 2018. 262, 06002. DOI: 10.1051/mateconf/201926206002.
- [33] Fomichev, S.V., Dergacheva, N.P., Babievskaya, I.Z., Noskova, O.A. & Krenev, V.A. (2013). Use of highly dispersed basalt powder for manufacturing stone ceramics. *Theoretical Foundations of Chemical Engineering*, 47, 626-628. DOI: 10.1134/S0040579513050023.
- [34] Fomichev, S.V., Dergacheva, N.P., Steblevskii, A.V. & Krenev, V.A. (2011). Production of ceramic materials by the sintering of ground basalt. *Theoretical Foundations of Chemical Engineering*, 45(4), 526-529. DOI: 10.1134/S0040579510051124.
- [35] Dzhigiris, D.D., Makhova, M.F. (2002). *Osnovy proizvodstva bazal'tovykh volokon i izdelii [Frication fundamentals of basalt fibers and items]*. Moscow: Teploenergetik.
- [36] Kostikov, V.I., Smirnov, L.N. (2001). *Bazal'tovoloknistye materialy [Basalt fibrous materials]*. Collection of articles. Moscow: Informkonversiya.
- [37] Abdurakhmanov, S.A., Rashidova, R., Mamatkarimova, B. & Sattarov, L.K. (2015). About basalt production and ways to improve basalt product quality. *RMZ-materials and geoenvironment*. 62(2), 133-139.
- [38] Drobot, N.F., Noskova, O.A., Steblevskii, A.V., Fomichev, S.V. & Krenev, K.A. (2013). Use of chemical and metallurgical methods for processing of gabbro - basalt raw material. *Theoretical Foundations of Chemical Engineering*. 47(4), 484-488. DOI: 10.1134/S004057951304 0052.
- [39] Baisanov, S.O., Tolymbekov, M.Zh., Zharmenov, A.A., Chekimbaev, A.F. & Terlikbaeva, Zh. (2008). Using clay rock in smelting ferrosilicoaluminum. *Steel in Translation*. 38(8), 668-670.
- [40] Shevko, V.M., Karatayeva, G.E., Amanov, D.D., Badikova, A.D., Bitanova, G.A. (2019). Joint Production of Calcium Carbide and A Ferroalloy of The Daubaba Deposit Basalt. *International Journal of Mechanical Engineering and Technology (IJMET)*. 10(2), 1187-1197.
- [41] Shevko, V.M., Badikova, A.D., Karataeva, G.E. & Tuleev, M. A. (2019). Extraction Kinetics of Silicon, Aluminum, and Calcium from Dubersay Basalt by Electric Smelting. *International Journal of Engineering and Advanced Technology*. 8, 4566-4570.
- [42] Shevko, V. M., Karataeva, G. E., Badikova, A. D., Amanov, D. D. & Tuleev, M. A. (2018). Termodinamicheskaya model' vliyaniya temperatury i ugleroda na poluchenie ferrosplava i karbida kal'tsiya iz bazal'ta mestorozhdeniya Dubersai [Thermodynamic model of temperature and carbon effect on production of ferrous alloy and calcium carbide from Dubersai basalt]. *Kompleksnoe ispol'zovanie mineral'nogo syr'ya*. 3, 86-94.
- [43] Shevko, V.M., Zharmenov, A., Aitkulov, D.K., Terlikbaeva, A., Badikova, A.D. & Karataeva, G.E. (2019). Elektrotermicheskoe poluchenie ferrosplava i karbida kal'tsiya iz domennogo shlaka [Electrochemical production of ferrous alloy and calcium carbide from blast furnace slag]. *Promyshlennost' Kazakhstana*. 2, 81-85.
- [44] Roine, A., Jarkko-Mansikka-aho, Kotiranta, T., Bjorklund, P., Lamberg, P. (August 14, 2006). HSC Chemistry 6.0 User's Guide. Outotec Research Oy.

- [45] Steel chips, price. MetalTorg.Ru Information agency. News, analytics, market statistics of ferrous, non-ferrous, and precious metals. Retrieved June 28, 2020, from <https://www.metaltorg.ru/stalnaya-struzhka-tsen.htm>
- [46] Products of Iron Concentrate Company. Iron Concentrate Company. Retrieved June 28, 2020, from <http://icckaz.com/ru/node/39>
- [47] Shevko, V.M., Serzhanov, G.M., Karataeva, G.E., Amanov, D.D. (2019). Computation of equilibrium distribution of elements with regard to HSC-5.1 software. Computer program. RK Certificate №1501.
- [48] Shevko, V.M., Amanov, D.D., Karataeva, G.E. & Aitkulov, D.K. (2016). Kinetika polucheniya kompleksnogo ferrosplava iz kremnii-alyuminiisoderzhashchei opoki [Kinetics of production of integrated ferrous alloy from silicon and aluminum containing mold frame]. *Mezhdunarodnyi zhurnal prikladnykh i fundamental'nykh issledovaniy*. 10-2, 194-196.
- [49] Kozlov, K.B., Lavrov, B.A. (2011). *Poluchenie karbida kal'tsiya v dugovoi pechi i ego analiz* [Production of calcium carbide in arc furnace and its analysis]. St. Petersburg: State Technological Institute.
- [50] State standard GOST 1460-2013. Calcium carbide. Specifications. (2014). Moscow: Standartinform.
- [51] Ahmad, Z., Yasin, M., Nadeem, S. & Manzoor Atta, B. (2003). Effect of Application of Calcium Carbide on Growth of Cotton Crop. *Asian Journal of Plant Sciences*. 2, 569-574.
- [52] Thompson, R. B. (1996). Using calcium carbide with the acetylene inhibition technique to measure denitrification from a sprinkler irrigated vegetable crop. *Plant Soil*. 179, 9-16.
- [53] Podzolic soils. Big Encyclopedic Dictionary. Agriculture. Retrieved June 28, 2020, from <http://www.cnsnb.ru/AKDIL/0024/base/RP/003410.shtm>
- [54] Makarenko, L.N. (1996). Primenenie pod ogurtsy karbida kal'tsiya [Calcium carbide for cucumbers]. *Izvestiya TSKhA*. 3, 111-114.
- [55] Specifications TU 0820-011-14513884-2013. Aluminum ferrosilicon. (2013). Ekaterinburg: UIS.